Student Conference Proceedings
Vol 2, No 1, 2026, Article ID 2646, 4 Pages

Student Conference Lübeck

Proceedings Article

Wavelength dependent Raman spectroscopy on chemical warfare agent (CWA) simulants

Anastasia Strocacenco[a,b*] · Patrick Di Martino-Fumo[b] · Lisa B. Dreier[b*]

[a]Study program Biophysics, Universität zu Lübeck, Lübeck, Germany
[b]Institute of Technical Physics, German Aerospace Center (DLR), Hardthausen, Germany
*Corresponding author, email: anastasia.strocacenco@.uni-luebeck.de; lisa.dreier@dlr.de

Received 27 April 2026; Accepted 10 July 2026; Published online 25 August 2026

Abstract

This study investigates the potential of Raman spectroscopy for the detection of four chemical warfare agent (CWA) simulants - Glyphosate, Triphenyl phosphate, Triethyl phosphate and Tributyl phosphate, using multiple excitation wavelengths. The aim of this work is to evaluate the influence of excitation wavelength on spectral quality and the practical usability of different Raman setups for CWA-related measurements. The results demonstrate a strong wavelength dependence of the Raman signal intensity, with shorter excitation wavelengths being less suitable for fluorescent analytes due to background radiation that can obscure characteristic Raman bands. These findings support the selection and optimization of excitation wavelengths for reliable Raman-based identification of CWAs.

I. Introduction

Chemical warfare agents (CWAs) have been used on multiple occasions during terroristic attacks and wars throughout history and remain a serious danger to the population due to their high toxicity and life-threatening effect. These substances have either lethal or incapacitating effects on humans and can be classified according to their physiological effect. CWAs include nerve agents, vesicants, blood agents, chocking agents and others [1], [2]. In order to prevent possible attacks and protect the population, sensitive and reliable detection possibilities are needed to identify hazardous chemicals. A direct experimental investigation of the CWAs is very difficult because of their high toxicity and associated restrictions on their laboratory use. The common procedure in this case is to use so-called simulants, which exhibit similar physical and chemical properties to CWAs, such as vapor pressure and relevant functional groups, but are hundreds of magnitudes less toxic [3].

Several technologies have already been developed to identify hazardous chemicals, such as ion mobility spectrometry, colorimetric and fluorimetric methods. However, all these methods deviate from ideal due to limitations such as cost, sensitivity, specificity and especially detection distance [4]. In this context, Raman spectroscopy offers a significant advantage as a non-contact technique which can be performed in standoff mode. It is based on the inelastic scattering of incident light resulting from its interaction with molecular vibrations. The observed Raman spectrum arises from scattered light whose frequency differs from that of the incident radiation. The resulting spectrum is molecule specific and can serve as a unique molecular "fingerprint" [5]. Most of the Raman instruments nowadays employ near-infrared excitation to reduce fluorescence background and sample absorption that are more pronounced at shorter wavelengths. However, ultraviolet excitation wavelengths offer some advantages, particularly in significantly increasing the Raman signal, which is proportional to $\frac{1}{\lambda^4}$, and enabling resonance enhancement [5].

In this article, four CWA-simulants, namely Glyphosate (GPH), Triphenyl phosphate (TPP), Triethyl

10.18416/SCP.2026.2646

phosphate (TEP) and Tributyl phosphate (TBP) have been investigated using three Raman setups operating at different excitation wavelengths in the near infrared and ultraviolet regions. Raman band positions of all simulants were compared with literature values and a comparison of all obtained data based on excitation wavelength was qualitatively performed.

II. Materials and Methods

For this study, the following substances were used: Glyphosate powder (GPH, ≥ 99 %, CAS-number: 1071-83-6, Sigma-Aldrich), Triphenyl phosphate powder (TPP, ≥ 99 %, CAS-number: 115-86-6, Sigma-Aldrich), Triethyl phosphate liquid (TEP, ≥ 99 %, CAS-number: 78-40-0, Millipore), Tributyl phosphate liquid (TBP, ≥ 99 %, CAS-number: 126-73-8, Sigma-Aldrich) and ethanol (≥ 99.5 % CAS-number: 64-17-5, Millipore).

II.I. Fluorescence measurements

Fluorescence and absorbance measurements were performed using a FS5 v2 spectrofluorometer (Edinburgh Instruments). GPH, TPP, TBP and TEP were dissolved in ethanol at a concentration of 10^{-3} M and measured in 10 mm path length UV quartz cuvettes (Hellma Analytics). Fluorescence emission spectra were recorded from 270 to 850 nm with an excitation wavelength of 266 nm, an offset slit of 1 nm and a scan slit of 1 nm, using a dwell time of 0.2 seconds and 1 nm wavelength steps. For absorbance measurements, transmission spectra were collected in the range of 200 to 850 nm, after which absorbance spectra were automatically calculated by the instrument.

II.II. Raman measurements

785 nm excitation - for the Raman measurements with an excitation wavelength of 785 nm, a portable Raman-Spectrometer MIRA XTR (Metrohm) was used. Spectra were collected from 400 to 2300 cm^{-1} with a spectral resolution of 17 cm^{-1} (FWHM). The measurements were performed in auto mode, the acquisition time and number of accumulations were thus chosen automatically by the instrument to obtain an ideal signal-to-noise ratio (SNR). The integration time and number of accumulations varied between the samples. The laser output power was set to 50 mW and the detection distance was constant at 5 mm. TPP, TEP and TBP were measured in bulk using 20 mm path length vials, which were placed in the instrument's dedicated vial holder. GPH powder was measured after ethanol washing and centrifugation (15,000 rpm, 5 min) in Eppendorf tubes using a universal attachment with a 5 mm focal point.

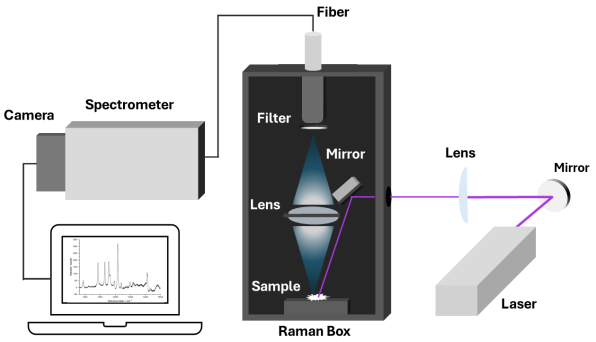

Figure 1: Schematic diagram of Raman setup with a 355 nm excitation wavelength. The components are not shown to scale.

266 nm excitation - the Raman measurements with 266 nm excitation wavelength were performed using an inhouse-built setup with a Q-switched solid state UV laser (CryLas GmbH, FQSS 266-Q) with a wavelength of 266 nm, a repetition rate of 1 kHz, a pulse width of 1 ns and a pulse energy of 12 µJ. The detection distance was fixed at 75 cm. The detailed description of the setup can be found in [6]. The spectral resolution of the setup was 33 cm^{-1} (FWHM). Spectra were recorded from 306 to 2031 cm^{-1}, averaging 25 frames with 800 accumulations and a detector gain of 5. All of the substances were measured in 2 mm path length cuvettes, TEP and TBP were additionally measured in 10 mm path length cuvettes.

355 nm excitation - for Raman measurements with an excitation wavelength of 355 nm a new Raman setup, which is schematically shown in Figure 1, was built. The setup was equipped with a diode-pumped solid state (DPSS) laser (Frankfurt Laser Company) with a 355 nm excitation wavelength, a repetition rate of 20 kHz and a pulse energy of 5 µJ. The focused laser beam was directed into a 3D printed Raman box, where the excitation light was directed onto the sample via a 45° mirror. The backscattered light was collected with a biconvex lens with a diameter of 12.7 mm and a focal length of 40 mm, spectrally filtered and coupled into a round-to-linear fiber bundle consisting of 19 individual fibers, each with a core diameter of 200 µm. The detection distance was fixed at 9 cm. The linear end of the fiber was connected to the SpectraPro HRS-500 spectrometer (Princeton Instruments) with a slit width of 500 µm and the detection was achieved via a PI-MAX4 iCCD camera with a chip size of 1024x253 pixel, gate delay of 250 ns and gate width of 1 ms. The spectral resolution of the setup was 11 cm^{-1} (FWHM). Spectra were recorded from 500 to 4000 cm^{-1} using a step-and-glue method with one frame, 1500 accumulations and a detector gain of 5. TEP and TBP liquids were measured in a 10 mm path length cuvette and GPH and TPP powders were directly placed into a sample holder of the Raman box. All the spectra were smoothed to improve peak identification.

All spectra were analyzed using Origin 2024b. The

10.18416/SCP.2026.2646

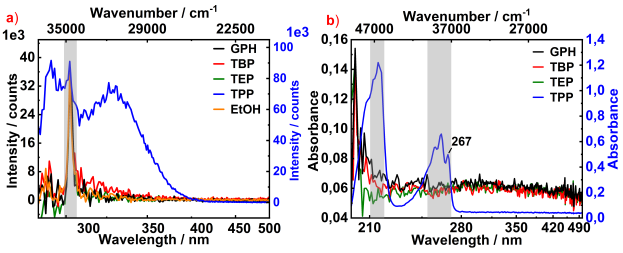

Figure 2: Emission (a) and absorption (b) spectra of the CWA-simulants TEP, TBP, GPH and TPP. Additionally, the emission spectrum of pure ethanol is shown. Emission intensities and absorbance of TEP, TBP and GPH are referenced to the left y-axis, whereas the emission intensity and absorbance of TPP is referenced to the right y-axis. The bottom x-axis shows the wavelength in nm and the top x-axis indicates the corresponding wavenumber in cm^{-1}.

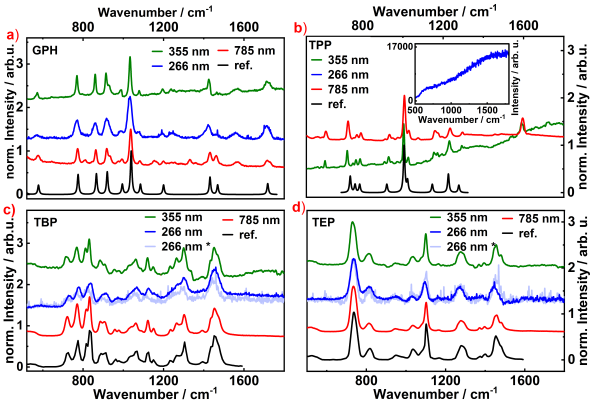

Figure 3: Raman spectra of GPH (a), TPP (b), TBP (c) and TEP (d) using an excitation wavelength of 785 nm (red), 355 nm (green) and 266 nm (blue). The corresponding literature spectra (black) are shown on each graph [8], [9], [10], [11]. Each of the substances was measured in bulk in their natural state (powder or liquid). All spectra of GPH, TBP and TEP measured at excitatiton wavelengths of 266, 355 and 785 nm as well as spectra of TPP obtained with 355 and 785 nm excitation wavelengths were normalized to their respective maximum and vertically offset for clarity. The spectrum of TPP using excitation wavelength of 266 nm was not normalized and is displaced in inset. The TBP and TEP spectra with 266 nm excitation were measured at two different path lengths 10 mm and 2 mm (*).

reference spectra of TPP and GPH were digitized using a python script and those of TEP and TBP using WebPlotDigitizer automeris [7].

III. Results and Discussion

III.I. Fluorescence measurements

Fluorescence measurements were conducted to gain a first characterization of the spectral behavior of the samples. Emission spectra of TEP, TBP, TPP and GPH are shown in Figure 2 a. All four samples exhibit a peak at 288 nm that originates from the intrinsic fluorescence of the quartz cuvette, which is also seen in the emission spectrum of ethanol (Figure 2 a). Only TPP additionally shows two strong and broad fluorescence bands between 270 and 290 nm and between 300 nm and 350 nm which are discussed in detail in the section III.II. Raman measurements. The absorbance spectra of TEP, TBP, TPP and GPH are shown in Figure 2 b. TBP, TEP and GPH do not exhibit any significant absorbance in the measured spectral range. In contrast, TPP shows four distinct absorbance peaks at 215 nm, 256 nm, 261 nm and 267 nm.

III.II. Raman measurements

Each of the simulants was measured using three different Raman setups with varying excitation wavelengths (266, 355 and 785 nm). The results and the associated reference spectra are shown in Figure 3.

Figure 3 a shows the spectra of GPH powder. All major Raman bands of GPH in the region between 520 and 1800 cm^{-1} are observed for all excitation wavelengths [8]. Minor variations in peak widths were observed among the different experimental setups. This variation is most pronounced in the spectrum obtained with 266 nm excitation wavelength, where a single band is observed at approximately 913 cm^{-1}, whereas the other excitation wavelengths exhibit an apparent overlap of two bands at this position. This difference arises from the lower spectral resolution of the setup with 266 nm excitation but does not affect the identification of the main vibrational modes.

The Raman spectra of TPP powder are shown in Figure 3 b. For the excitation wavelengths with 355 and 785 nm, all major TPP Raman bands are observed between 520 and 1800 cm^{-1} [9]. The spectrum obtained with 266 nm excitation wavelength is shown in the inset. This spectrum shows a strong fluorescence of the sample. This observation is also supported by the absorbance measurement, which is seen in Figure 2 b where a peak at 267 nm is observed. The behavior of the substance is strongly correlated with its chemical structure. TPP consists of three phenyl rings, which strongly absorb in the UV region, making the Raman bands difficult to identify at this particular excitation wavelength. Fluorescence is also present in the spectrum recorded with 355 nm excitation wavelength; however, it is less intense and does not hinder the identification of the Raman bands. In contrast, no fluorescence was detected with 785 nm excitation wavelength. These results indicate that reliable Raman spectra of TPP can be obtained with an excitation wavelength above 270 nm without interference from absorption (Figure 2 b).

The results for TBP liquid are demonstrated in Figure 3 c. All spectra show Raman bands characteristic

10.18416/SCP.2026.2646

for TBP in the region between 520 and 1800 cm^{-1} [10]. The influence of the path length of the cuvette on the SNR was analyzed. Despite the lower SNR of the measurement with 2 mm path length cuvettes, the Raman peaks are clearly visible, making it possible to also identify the sample if only low amounts are present. This is a first step toward demonstrating the suitability of Raman spectroscopy for future standoff detection of hazardous materials with a smaller amount of the sample.

The spectra of TEP liquid are shown in Figure 3 d. All important Raman bands in the region between 520 and 1800 cm^{-1} are seen in all spectra and can be assigned to TEP [11]. The results are comparable to those obtained for TBP and show that 2 mm path length cuvettes yield a lower SNR, nevertheless, the Raman bands remain clearly visible.

In this paper a comparative analysis of all spectra was performed; however, a direct and quantitative comparison between the spectra is challenging because the systems differ substantially, particularly in their optical design, the optics employed, the spectrometer resolution and the respective detection distances. Nevertheless, an initial impression of the suitability of the individual excitation wavelengths for detecting Raman signals could be obtained.

IV. Conclusion

In this work a comparison of CWA simulant detection with Raman spectroscopy using three different excitation wavelengths (266, 355 and 785 nm) was performed. The obtained Raman bands of GPH, TPP, TBP and TEP correlated well with literature band positions. Characteristic Raman bands were visible in all spectra except when masked by strong fluorescence as for TPP excited at 266 nm. Due to different spectral resolutions and detection distances of the three setups, the SNR and the peak width varied slightly across all spectra. The highest SNR was obtained with 785 nm excitation, which has also the smallest detection distance. The broadest spectra were seen in the measurements with 266 nm excitation wavelength due to slightly lower resolution of the spectrometer. Additionally, TEP and TBP were measured in cuvettes with different optical path lengths to investigate the effect of path length on signal quality. The results show that the noise level increases as the sample amount decreases.

In summary, these encouraging results give a first impression on the potential of Raman spectroscopy for CWA detection. In general, almost all substances were successfully detected with the three excitation wavelengths. However, shorter wavelengths were found to be less suitable due to fluorescence interference, especially 266 nm excitation. To better simulate realistic scenarios and further evaluate the applicability of the method, more measurements at different substance concentrations and on various background materials are required. Such measurements can also be used to determine the detection limit at different excitation wavelengths.

Acknowledgments

The work has been carried out at the Institute of Technical Physics in Hardthausen, German Aerospace Center (Deutsches Zentrum für Luft- und Raumfahrt) and supervised by Prof. Dr. Christian Hübner, Institute of Physics, Universität zu Lübeck. Sincere gratitude is expressed to the Department of Atmospheric Propagation and Effect for providing the opportunity to complete the internship at their institution. Additional thanks to Björn Prietzel for his assistance with the chemicals.

Author's statement

Conflict of interest: Authors state no conflict of interest.

References

[1] T. James, S. Wyke, and et al. Chemical warfare agent simulants for human volunteer trials of emergency decontamination: A systematic review. *Journal of Applied Toxicology*, (38)pp. 113–121, 2017, doi:10.1002/jat.3527.

[2] K. Ganesan, S. Raza, and R. Vijayaraghavan. Chemical warfare agents. *Journal of Pharmacy and Bioallied Sciences*, (3)pp. 166–78, 2010, doi:10.4103/0975-7406.68498.

[3] J. Lavoie, S. Srinivasan, and R. Nagarajan. Using cheminformatics to find simulants for chemical warfare agents. *Journal of Hazardous Materials*, (194)pp. 85–91, 2011, doi:10.1016/j.jhazmat.2011.07.077.

[4] R. Sferopoulos, A Review of Chemical Warfare Agent (CWA) Detector Technologies and Commercial-Off-The-Shelf Items. Human Protection and Performance Division, 2009, eprint: ark:/13960/t7kq51d1d.

[5] A. Hobro and B. Lendl. Stand-off raman spectroscopy. *TrAC Trends in Analytical Chemistry*, (11), 2009, doi:10.1016/j.trac.2009.08.008.

[6] F. Duschek, P. di Martino-Fumo, and et.al. Vibrational spectroscopy for the standoff detection of organic phosphorous agents on realistic background material. *SPIE Digital Library*, 14048, 2026, doi:https://doi.org/10.1117/12.3094455.

[7] A. Rohatgi, Webplotdigitizer, version 5.2. URL: https://automeris.io.

[8] L. Mikac, I. Rigó, and et al. Comparison of glyphosate detection by surface-enhanced raman spectroscopy using gold and silver nanoparticles at different laser excitations. *MDPI Molecules*, (18), 2022, doi:10.3390/molecules27185767.

[9] L. Cantu and E. Gallo. Explosives and warfare agents remote raman detection on realistic background samples. *The European Physical Journal Plus*, 137(207), 2022, doi:https://doi.org/10.1140/epjp/s13360-022-02416-0.

[10] N. I. of Advanced Industrial Science and Technology, Accessed: 2026-01-12, 1999. URL: https://sdbs.db.aist.go.jp/CompoundLanding.aspx?sdbsno=2905.

[11] N. I. of Advanced Industrial Science and Technology, Accessed: 2026-01-12, 1999. URL: https://sdbs.db.aist.go.jp/CompoundLanding.aspx?sdbsno=2164.